Removal of the Pro-Domain Does Not Affect the Conformation of the Procaspase-3 Dimer†

Cristina Pop,‡ Yun-Ru Chen,‡ Brandye Smith,§ Kakoli Bose,‡ Benjamin Bobay,‡ Ashutosh Tripathy,|| Stefan Franzen,§ and A. Clay Clark*,‡

Department of Molecular and Structural Biochemistry and Department of Chemistry, North Carolina State University, Raleigh, North Carolina 27695, and Macromolecular Interactions Facility, University of North Carolina at Chapel Hill, Chapel Hill, North Carolina 27599

Received May 21, 2001; Revised Manuscript Received August 13, 2001

ABSTRACT: We have investigated the oligomeric properties of procaspase-3 and a mutant that lacks the pro-domain (called pro-less variant). In addition, we have examined the interactions of the 28 amino acid pro-peptide when added in trans to the pro-less variant. By sedimentation equilibrium studies, we have found that procapase-3 is a stable dimer in solution at 25 °C and pH 7.2, and we estimate an upper limit for the equilibrium dissociation constant of ∼50 nM. Considering the expression levels of caspase-3 in Jurkat cells, we predict that procaspase-3 exists as a dimer in vivo. The pro-less variant is also a dimer, with little apparent change in the equilibrium dissociation constant. Thus, in contrast with the long pro-domain caspases, the pro-peptide of caspase-3 does not appear to be involved in dimerization. Results from circular dichroism, fluorescence anisotropy, and FTIR studies demonstrate that the pro-domain interacts weakly with the pro-less variant. The data suggest that the pro-peptide adopts a β-structure when in contact with the protein, but it is a random coil when free in solution. In addition, when added in trans, the pro-peptide does not inhibit the activity of the mature caspase-3 heterotetramer. On the other hand, the active caspase-3 does not efficiently hydrolyze the pro-domain at the NSVD^9 sequence as occurs when the pro-peptide is in cis to the protease domain. Based on these results, we propose a model for maturation of the procaspase-3 dimer.

Caspase activation, more than any other event, defines a cellular response to apoptosis [see review by Earnshaw (*1*)]. Caspases are a family of cysteinyl proteases that have an unusual requirement for aspartate at the P1 position in the substrate. Although many proteins are cleaved during apoptosis, caspases cleave key structural components of the cytoskeleton and nucleus as well as numerous proteins in signaling pathways, DNA repair or degrading enzymes, and transcription factors (*1*). In addition, caspases degrade amyloid precursor protein, presenilins, tau, and huntington, suggesting that they may have a role in neurodegenerative diseases (*2*). In short, caspase activation results in an irreversible, organized dismantling of the cell.

Currently, 14 caspases have been identified (*3*), and it is generally accepted that caspase-3 (CPP32, apopain, Yama) is the primary executioner during apoptosis (*4, 5*). The mature, enzymatically active caspase-3 is a tetramer with a M_r of approximately 60 000 and consists of two copies of one large (α) and one small (β) subunit, described as dimers of heterodimers, $(\alpha\beta)_2$ (*6, 7*). Interestingly, the two subunits in the ($\alpha\beta$) heterodimer form a single domain, which consists of a six-stranded β-sheet core flanked by α-helices. Each ($\alpha\beta$) heterodimer contains an active site, although the heterodimer appears to be inactive (*8*). While the catalytic dyad (Cys163, His121) is contributed by the large subunit, both subunits contribute residues that form the S1−S4 binding pockets (*7*). All other caspases for which the crystal structure is known (caspases-1, -7, and -8) display a similar fold (*9*−*11*), demonstrating the structural homology within the family.

Like the other caspases, caspase-3 exists in normal cells as an inactive zymogen and must be activated by proteolytic processing. While the three-dimensional structures have not been determined, procaspases are organized with an amino-terminal pro-domain, which varies in size and function, followed by the large subunit, an optional intersubunit linker, and the small subunit, as shown in Figure 1. Although processing appears to be more complicated for long pro-domain caspases, in general, caspases are activated in a two-step sequential process (*12*). For procaspase-3, the first cleavage occurs at Asp175 (*13*), which separates the covalent linkage between the large and small subunits. The small subunit remains associated through noncovalent interactions. The cleavage at Asp175 generally occurs by an upstream activator caspase. Based on the increase in enzyme activity (*14*) as well as other biochemical data (*15, 16*), significant conformational rearrangements must occur as a result of the first cleavage. In the second step, the pro-domain is auto-

† This work was supported by a grant from the American Diabetes Association.

* To whom correspondence should be addressed at the Department of Molecular and Structural Biochemistry, 128 Polk Hall, North Carolina State University, Raleigh, NC 27695-7622. Phone: (919) 515-5805. Fax: (919) 515-2047. E-mail: clay_clark@ncsu.edu.

‡ Department of Molecular and Structural Biochemistry, North Carolina State University.

§ Department of Chemistry, North Carolina State University.

|| Macromolecular Interactions Facility, University of North Carolina at Chapel Hill.

10.1021/bi011037e CCC: $20.00
Published on Web 10/30/2001

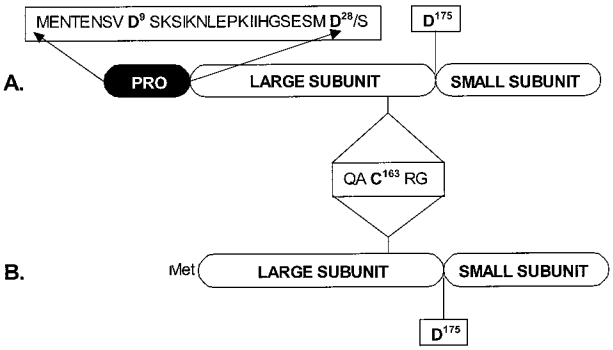

FIGURE 1: Procaspase-3 and pro-less variant. (A) Schematic representation of full-length procaspase-3, showing the pro-domain sequence, the conserved catalytic motif, and the cleavage sites, D9, D28, and D175. (B) Procaspase-3 lacking the 28 amino acid propeptide, referred to in the text as 'pro-less variant'.

catalytically removed from the large subunit (*13*) by a rapid proteolysis at Asp9 (see Figure 1) followed by a slow cleavage at Asp28 (*14*). The activity of the protein following cleavage at Asp9 ($NSVD^{9}/S$) appears indistinguishable from that of the mature heterotetramer (*14*), in which the N-terminus begins at Ser29 ($ESMD^{28}/S$). The significance of the two cleavage sites within the pro-domain is not yet understood, but many of the procaspases contain more than one processing site in the pro-domain (*17*).

In the case of procaspase-1 and other long pro-domain caspases, the pro-domain (119 amino acids) is involved in dimerization of the procaspase, leading to autoprocessing. This is due to the presence of a dimerization motif within the pro-domain. Procaspase-1, for example, contains a caspase recruitment domain (CARD) within the first 92 amino acids of the pro-domain. The CARD is a six-helix bundle folding motif and is responsible for highly specific interactions between the procaspase and homologous CARD motifs in adapter proteins (*18*).

Dimerization represents an early event in maturation of procaspase-1 (*19*). For downstream caspases, such as caspase-3, there is no evidence that dimerization is an early event. Indeed, procaspase-3 is frequently drawn as a monomer in the literature reviews (*20*), although the oligomeric properties have not been examined. Thus, the role of the pro-domain, if any, in dimerization and maturation of the short pro-domain procaspases is less clear. In addition, the pro-domain (28 amino acids) does not inhibit the protease activity when present in cis of the mature heterotetramer (*14*), suggesting the possibility that the short pro-domain of executioner caspases represents a vestigial linker between the CARD motif and the amino terminus of the large subunit. Indeed, procaspase-1 contains 27 amino acids between the CARD motif and the large subunit. However, recent data argue that the short pro-domain may also have a function in maturation. Recombinant procaspase-3 has been shown to autoprocess during overexpression in *E. coli*, yeast, and insect cells or during purification after overexpression in mammalian cells (*7*, *21*−*23*), suggesting that the pro-enzyme forms oligomers at high concentrations, facilitating autoprocessing. Recently, Meergans and co-workers (*24*) demonstrated that caspase-3 constructs lacking the pro-domain were able to autoprocess in HeLa cells, in contrast with the intact precursors. Thus, the pro-sequence may not inhibit the activity of the active protease, but rather may function somehow as an additional control to decrease the low levels of procaspase activity, preventing spontaneous activation.

Because of these considerations, we have investigated the oligomeric state of procaspase-3 and the role of the pro-domain on procaspase-3 stability and caspase-3 activity. We have used a catalytically inactive mutant (C163S) of the full-length human procaspase-3 as well as a variant of procaspase-3(C163S) in which the pro-domain is removed, referred to as the pro-less variant[1] (see Figure 1). We show here that procaspase-3(C163S) is a dimer in solution at 25 °C, and based on these data as well as estimations of the procaspase-3 concentration in vivo, we suggest that the protein is a dimer in vivo. Removal of the pro-domain has no effect on the oligomeric or conformational properties of procaspase-3. In addition, we demonstrate that the pro-domain interacts with the pro-less variant in trans, suggesting that the pro-peptide may bind weakly to the procaspase dimer at site(s) away from the active site region.

MATERIALS AND METHODS

Chemicals. Ampicillin, antifoam-C, bovine serum albumin, carbonic anhydrase, CHAPS, cytochrome *c*, DEAE-Sepharose, dansyl chloride, DMF, DMSO, DTT, EDTA, EGTA, glycerol, IPTG, kanamycin, nickel sulfate, PMSF, monobasic and dibasic potassium phosphate, Sephacryl-S15, Sephacryl-S100, sodium bicarbonate, TLCK, TPCK, and Trizma base were from Sigma. Ultrapure ammonium sulfate, guanidine hydrochloride, imidazole, and urea were from ICN. Sodium chloride was from Fisher. Tryptone and yeast extract were from Difco. His-bind resin was from Novagen. Potassium chloride and sucrose were from Mallinckrodt. Acetonitrile and HEPES were from Acros. α-Cyano-4-hydroxycinnamic acid was from Aldrich.

Plasmid Construction. The procaspase-3 gene was amplified by PCR from pET21b-CPP32 (*25*), kindly provided by Dr. Emad Alnemri, using the primers HC3P32F (GTCGCGGATCATATGGAGAACACTG) and HC3P12R (GTGGTGGTGGTGCTCGAGGTG). This introduced an *Nde*I site at the 5′ end of the gene and an *Xho*I site at the 3′ end of the gene. The amplified gene product was inserted into pET21b that had been digested with *Nde*I and *Xho*I. This strategy removed 14 amino acids at the amino terminus of procaspase-3 that arise from the vector in pET21b-CPP32. The resulting plasmid, pHC332, produces procaspase-3 with the correct amino terminus. The active site cysteine (Cys163) was mutated to serine using QuickChange site-directed mutagenesis kit (Stratagene), with the primers HCP3CS1 (5′-CATTATTCAGGCCT**C**CCGCGGTACAGAACTGGACTGTGG-3′) and HCP3CS2 (5′-CAGTTCTGTACCGCGG**G**AGGCCTGAATAATGAAAAGTTTGG-3′), and plasmid pET21b-CPP32. This strategy also introduced a unique *Sac*II

[1] Abbreviations: Pro-less variant, procaspase-3 (C163S) lacking the pro-domain; CHAPS, 3-[(3-chloroamidopropyl)dimethylammonio]-1-propanesulfonate; DMSO, dimethyl sufoxide; DMF, *N*,*N*-dimethylformamide; HEPES, 4-(2-hydroxyethyl)-1-piperazineethanesulfonic acid; IPTG, isopropyl β-D-thiogalactopyranoside; PMSF, phenylmethylsulfonyl fluoride; SDS−PAGE, sodium dodecyl sulfate−polyacrylamide gel electrophoresis; TFA, trifluoroacetic acid; TLCK, *N*-α-*p*-tosyl-L-lysine chloromethyl ketone; TPCK, *N*-tosyl-L-phenylalanine chloromethyl ketone; Z-VAD-FMK, *N*-benzyloxycarbonyl-Val-Ala-Asp-fluoromethyl ketone; Z-DEVD-AFC, *N*-benzyloxycarbonyl-Asp-Glu-Val-Asp-7-amino-4-trifluoromethyl coumarin.

site (underlined) downstream of the C163S mutation (shown in boldface type). Plasmids were first screened by digestion with *Sac*II, and positive clones were sequenced to confirm the mutation. The mutated gene was cloned into pET21b, as described above, to produce the plasmid pHC33201.

Plasmid pHC32901 was constructed by subcloning the DNA for the procaspase-3 large and small subunits from pHC33201. The primers for PCR amplification were HC3P17F (5′-GCGAATCACATATGTCTGGAATATCCC-3′) and HC3P12R (5′-GTGGTGGTGGTGCTCGAGGTG-3′), generating *Nde*I and *Xho*I sites at the 5′ and 3′ ends, respectively. The ∼750 bp fragment was inserted into pET21b digested with *Nde*I and *Xho*I. The resulting proteins [pro-caspase-3(C163S) and pro-less variant] have carboxyl termini consisting of the sequence Leu-Glu-His_6 that arise from the vector.

Plasmids pHC317 and pHC312, which harbor the genes for the caspase-3 large and small subunits, respectively, were constructed by subcloning the DNA corresponding to each subunit from pHC332, described above, into pET21b. The PCR primers for the large subunit were HC3P17F and HC3P17R (5′-CATCATCAACCTCGAGGTCTGTCTC-3′), whereas those for the small subunit were HC3P12F (5′-GCATTGAGCATATGAGTGGTGTTGATG-3′) and HC3P12R. In both cases, *Nde*I and *Xho*I sites were introduced at the 5′ and 3′ ends, respectively. All constructs were sequenced (both strands) in order to confirm the correct sequence.

Protein Purification. All steps were performed at 4 °C unless otherwise noted. The purification protocols are modifications of those described previously (*26*). In separate experiments, human procaspase-3(C163S) and the pro-less variant were purified as C-terminal-$(His)_6$-tagged proteins from *E. coli* BL21(DE3) harboring the plasmid pHC33201 or pHC32901, respectively. The protocols for purification of both proteins were similar. Cells were grown in Fernbach flasks containing 1 L of LB media with 50 μg/mL ampicillin and 0.003% antifoam-C at 30 °C. When the cultures reached an A_{600} of ∼1.2, protein expression was induced by the addition of IPTG to a final concentration of 0.1 mM. The cells were harvested after ∼16 h by centrifugation at 10000*g* for 15 min (GS-3 rotor). The bacterial pellets were resuspended in buffer A (50 mM Tris-HCl, pH 7.9, 100 μg/mL PMSF, 50 μg/mL TLCK, 100 μg/mL TPCK) (∼10 mL/L of culture) and lysed on ice using a French pressure cell (16 000 psi). The supernatant was separated from cell debris by centrifugation at 28000*g* for 30 min (SA-600 rotor). The pellet from this step was washed once with buffer A (5 mL/L of culture) and centrifuged for 30 min. The resulting supernatant was combined with the first. The proteins were fractionated between 30% and 80% ammonium sulfate, centrifuged at 22000*g* for 15 min, resuspended in buffer B (20 mM Tris-HCl, pH 7.9, 500 mM NaCl, 100 μg/mL PMSF, 50 μg/mL TLCK, 100 μg/mL TPCK) containing 5 mM imidazole, and dialyzed against the same buffer (2 × 80 volumes). The samples were then batch-bound for 2 min to His-bind resin (5 mL) equilibrated in buffer B containing 5 mM imidazole, and the resin was loaded onto a column (2 cm diameter). The resin was washed and the protein was eluted using step gradients of imidazole (20, 40, 100, 150, 250, and 500 mM imidazole in buffer B, 50 mL per step). The fractions were analyzed by SDS−PAGE (4−20% gradient gels) (*27*). For procaspase-3(C163S), the fractions containing the protein (150−250 mM imidazole) were pooled, concentrated (YM10 membrane), and dialyzed first against buffer C (50 mM Tris-HCl, pH 7.9, 250 mM NaCl, 1 mM EDTA, 1 mM EGTA) and then against buffer D (50 mM KH_2PO_4/K_2HPO_4, pH 7.5, 1 mM DTT, 1 mM EDTA, 1 mM EGTA) (2 × 80 volumes for both buffers). For the pro-less variant, the fractions from the His-bind resin containing the protein (100−250 mM imidazole) were pooled, concentrated (YM10 membrane), and dialyzed first against buffer E (50 mM KH_2PO_4/K_2HPO_4, pH 7.9, 250 mM KCl, 1 mM EDTA, 1 mM EGTA) and then buffer F (50 mM KH_2PO_4/K_2HPO_4, pH 7.5, 25 mM KCl, 1 mM DTT, 1 mM EDTA, 1 mM EGTA), respectively (2 × 80 volumes for both buffers). In each case, the sample was applied to a DEAE-Sepharose column (4 cm × 18 cm) that had been equilibrated with buffers D [procaspase-3(C163S)] or F (pro-less variant), respectively. The proteins were eluted at a flow rate of 4 mL/min with a linear gradient of 0−400 mM KCl [procaspase-3(C163S)] or 25−250 mM KCl (pro-less variant). Each fraction was tested using a mini-Bradford assay (*28*), and the positive fractions were analyzed by SDS−PAGE (4−20% gradient gels). The fractions (75−125 mM KCl) containing procaspase-3(C163S) or the pro-less variant (100−150 mM KCl) were pooled, concentrated, and dialyzed overnight against buffer D or buffer F, respectively. The proteins were stored at −80 °C. The protein purity was greater than 95% as assessed by SDS−PAGE.

The concentrations of procaspase-3(C163S) and the pro-less variant were determined using $\epsilon_{280} = 26\,500\ M^{-1}\ cm^{-1}$ and $\epsilon_{280} = 25\,300\ M^{-1}\ cm^{-1}$, respectively. The extinction coefficients were determined by the method of Edelhoch (*29*) and are in good agreement with that determined previously for procaspase-3 (*30*). The concentrations shown here are those of the monomers.

To generate the active caspase-3 heterotetramer, the subunits were purified separately and refolded together. Briefly, *E. coli* BL21(DE3) containing either pHC317 or pHC312 were grown at 37 °C in LB media. When the cultures reached an A_{600} of ∼1.2, protein expression was induced by the addition of IPTG to a final concentration of 0.1 mM. After 4 h of induction, the cells were harvested, resuspended in lysis buffer (20 mM Tris, pH 7.9, 500 mM NaCl), and broken in a French pressure cell as described above. The samples were centrifuged at 14 000 rpm for 30 min, and the insoluble portion was washed extensively with lysis buffer and dissolved in lysis buffer containing 6 M guanidine hydrochloride. The proteins were filtered (0.22 μm membrane) and purified by HPLC using a preparative C8 guard column (9.4 mm × 15 mm) and a preparative C18 column (21.2 mm × 250 mm; 300SB-C18) (Agilent Technologies). The flow rate was 1 mL/min. The column was developed with a linear gradient of 5% acetonitrile, 0.1% TFA to 85% acetonitrile, 0.1% TFA. The proteins eluted at 48% acetonitrile. The acetonitrile was removed by vacuum (1 h in a speedvac), and the proteins were dissolved in 20 mM Tris-HCl, pH 7.0, containing 6 M guanidine hydrochloride. The two purified subunits were mixed and refolded by rapid dilution in refolding buffer [100 mM HEPES, pH 7.5, 10% (w/v) sucrose, 0.1% (w/v) CHAPS, 0.5 M NaCl, 10 mM DTT] at 25 °C, as described previously (*6*). The final protein concentration was 8 μg/mL. To purify the

heterotetramer, the refolded protein was eluted from a size exclusion column (1 cm × 14 cm; Sephacryl S-100) with 50 mM KH_2PO_4/K_2HPO_4, pH 7.2, containing 1 mM DTT.

The active site concentration of caspase-3 was determined by enzymatic assay using the tetrapeptide substrate Z-DEVD-AFC (nonmethylated form) (Alexis) and titration with the irreversible inhibitor Z-VAD-FMK (CalBiochem), as described previously (*26*, *31*).

Analytical Ultracentrifugation. Sedimentation equilibrium experiments were performed at 25 °C in a Beckman XL-A ultracentrifuge equipped with absorbance optics and a four-hole AnTi60 rotor. The proteins were dialyzed at 4 °C into 50 mM KH_2PO_4/K_2HPO_4, pH 7.2, with either 1 mM DTT (280 nm data) or 0.05 mM DTT (230 nm data). The samples were equilibrated at three rotor speeds (14 000, 18 000, and 24 000 rpm), and the absorbance was measured at 280 or 230 nm. For the 280 nm data, the protein concentrations were as follows: (a) procaspase-3, 3.5, 9.4, and 18.9 μM; (b) pro-less variant, 1.26, 4.9, and 12.9 μM. For 230 nm, the protein concentrations were the following: (a) procaspase-3, 0.45, 0.78, 1.1, 3, and 4.1 μM; (b) pro-less form, 0.75, 1.25, 1.85, 2.5, and 3.7 μM. The experimental data were fit using the ORIGIN (*32*) version of the NONLIN algorithm (*33*) supplied by Beckman.

Fluorescence and Circular Dichroism Spectroscopy. Fluorescence emission was measured using a PTI C-61 spectrofluorometer (Photon Technology International). The excitation wavelength was either 280 or 295 nm, and fluorescence emission was measured from 300 to 400 nm. Circular dichroism was measured using a Jasco J600A spectropolarimeter using either a 0.1 cm (far-UV) or a 1 cm (near-UV) cell. All measurements were corrected for background signal. Both instruments were equipped with thermostated cell holders, and the temperature was held constant at 25 °C (±0.1 °C) using a circulating water bath.

Fluorescence Anisotropy. Labeled pro-peptide (1 μM), either wild-type or D9A mutant, was incubated at 25 °C in a buffer of 50 mM potassium phosphate, pH 7.5, 1 mM DTT in a final volume of 2 mL. The peptide was titrated with pro-less variant between 0 and 10 μM, and the fluorescence anisotropy was measured as described (*34*). The PTI C-61 spectrofluorometer in the T-based format was used (excitation wavelength of 345 nm and emission wavelength of 450 nm). The data were fit to a simple binding model as described (*35*).

Infrared Spectroscopy. FTIR spectra were collected by attenuated total reflection (ATR) spectroscopy using an ATR objective in a Bio-Rad UMA 500 infrared microscope equipped with a liquid nitrogen-cooled MCT detector and attached to a Bio-Rad FTS 6000 FTIR spectrometer. The ATR objective consists of a Ge crystal as the internal reflection element at the focus of a Cassagranian objective in a single-pass configuration. The sample was placed beneath the ATR objective, and spectra were recorded continuously as the sample was concentrated slowly by dehydration. This method presents an alternative means of determining the amide I line shape in H_2O. Previous studies on small amounts of sample in H_2O required cells with path lengths <6 μM. The details of the method and comparison with bench FTIR spectra are described elsewhere (*61*). The method has a number of advantages. Measurements can be made on small quantities of sample obtained in H_2O. Solvent exchange into D_2O is not required. Solvent subtraction is not typically required unless the protein appears to denature under the dehydration conditions. The state of the sample can be monitored continuously in order to verify that the spectrum is not changing during the experiment. Finally, the sample is fully recoverable.

The procaspase proteins and pro-peptide were concentrated to approximately 100 μM (~3 mg/mL procaspase, ~0.3 mg/mL pro-peptide) and dialyzed against a buffer of 20 mM potassium phosphate, pH 7.2, 1 mM DTT. Using a Wheaton automatic pipet, 20 μL of sample was injected onto a cylindrical sample well that is milled in a Teflon block. All protein spectra were recorded at room temperature as averages of 64 scans of the interferometer with a resolution of 2 cm^{-1}. Spectra were recorded immediately after the sample was deposited onto the Teflon block and continuously, as the samples were gently dehydrated using a steady stream of N_2 gas. Spectra were acquired until a protein gel had formed onto the Ge crystal. Background spectra were obtained subsequently. The Ge crystal was rinsed with H_2O and allowed to dry prior to loading another protein sample. The spectral data were acquired using the software package Win-IR-Pro v2.97 manufactured by Bio-Rad. Data analysis was performed using the software package Igor-Pro v3.1. The spectral range of 600−4200 cm^{-1} was used for protein analysis.

Enzyme Activity and Inhibition Studies. Activity measurements were carried out as described (*26*). Caspase-3 was diluted into enzyme assay buffer (50 mM HEPES, pH 7.4, 100 mM NaCl, 1 mM EDTA, 10% glycerol, 0.1% CHAPS, 10 mM DTT) and incubated at 25 °C for 5 min. The protein concentration was 10 times that used in the experiment. The enzyme was then added to enzyme assay buffer that contained the caspase-3-specific tetrapeptide substrate Z-DEVD-AFC. The final enzyme concentrations were 0.1, 1, or 10 nM, and the substrate concentration was 10 μM. In separate assays, an inhibitor (Z-VAD-FMK) was added so that the final concentrations ranged from 10 to 800 nM, as indicated in the figures. For all assays, the final volume was 200 μL. The fluorescence emission of AFC generated from the catalytic reaction was monitored for 5000 s using an excitation wavelength of 400 nm and an emission wavelength of 505 nm. The resulting fluorescence intensity curves were fit to eq 1 (*36*) for an irreversible inhibitor, where v_0 is the initial velocity, k_{obs} is the observed rate constant, and A is a baseline offset.

$$Fl = A + v_0[1 - \exp(-k_{obs}t)]/k_{obs} \quad (1)$$

The second-order rate constant for binding of inhibitor to enzyme was obtained from a plot of k_{obs}, determined from fits of the enzyme assay data to eq 1, versus inhibitor concentration.

The wild-type and mutant (D9A) pro-domains were synthesized by the Peptide Facility at the University of North Carolina at Chapel Hill. The peptides were dissolved in DMSO at a concentration of 100 mM. In separate enzyme assays, as described above, the pro-domains were added in place of the inhibitor so that the final concentration of pro-domain was between 0 and 500 μM. The final DMSO concentration was less than 0.5%, and had no effect on enzyme activity as determined in control experiments of

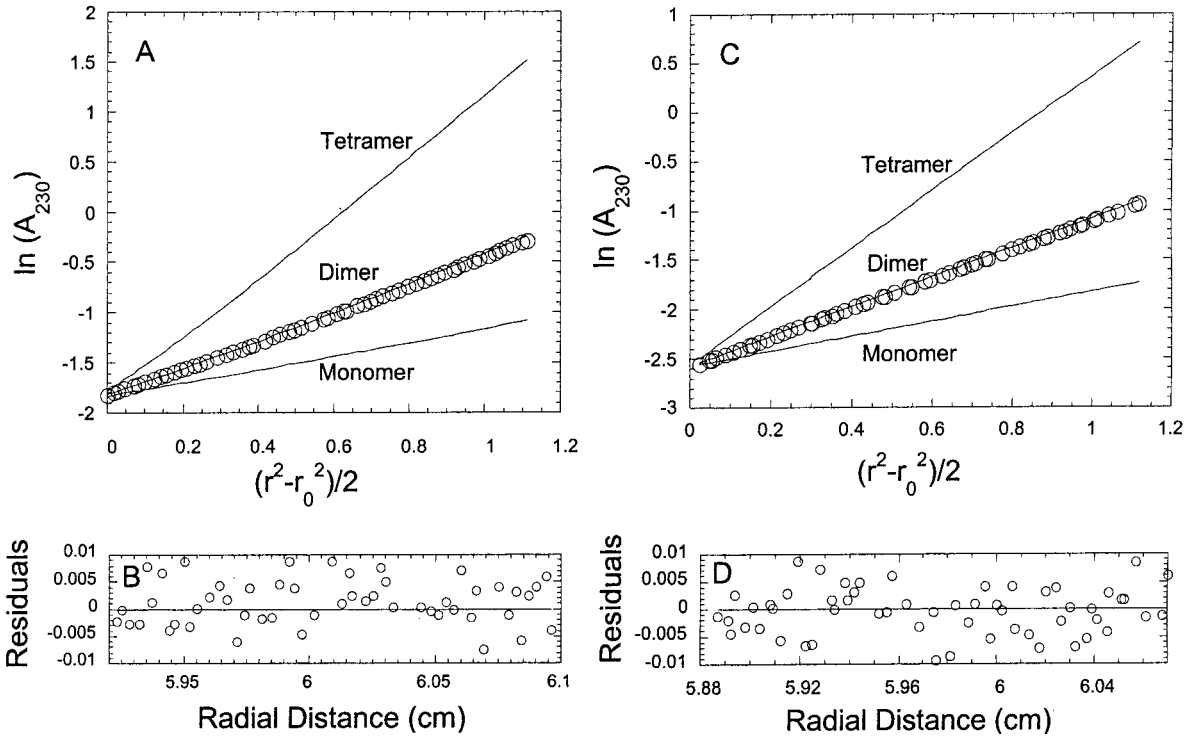

FIGURE 2: Sedimentation equilibrium studies of procaspase-3(C163S) and pro-less variant. Proteins (0.45−19.8 μM) were dialyzed against 50 mM KH_2PO_4/K_2HPO_4, pH 7.2, containing either 1 or 0.05 mM DTT. The spectra were recorded at 230 or 280 nm at 25 °C, using three rotor speeds (14 000, 18 000, and 24 000 rpm). The solid lines are the theoretical plots if the proteins were monomers, dimers, or tetramers, as indicated. The circles represent the experimental data for procaspase-3(C163S) (panel A) and pro-less variant (panel B). Residuals to the fits are shown in panels B and D.

enzyme in the presence of 0.5% DMSO. The enzymatic assays in the presence or in the absence of the pro-domain also were examined in a buffer containing 10% enzyme assay buffer, 10% water, and 80% 50 mM KH_2PO_4/K_2HPO_4, pH 7.2, 1 mM DTT, and were found to be nearly identical to those in enzyme assay buffer.

MALDI-TOF Mass Spectrometry. MALDI-TOF mass spectrometry was performed on a Bruker Proflex III equipped with a nitrogen laser (λ = 337 nm, 3 ns pulse width), deflection capabilities, delayed extraction, and an extended flight tube. The mass accuracy for analyte molecules is ±0.1% with external calibration. The matrix used was a saturated solution of α-cyano-4-hydroxycinnamic acid in acetonitrile, water, and TFA (50:50:0.1) (v/v/v). The instrument was calibrated against angiotensin I (1296.7 Da) and ubiquitin (8564.8 Da). Sample solutions (2 μL of 500 μM concentration) in 50 mM KH_2PO_4/K_2HPO_4, pH 7, with 1 mM DTT, containing 10% enzyme assay buffer, were desalted with Ziptip pipet tips (Millipore) and crystallized on a target plate with matrix solution (1:1). Experiments were performed at 25−30 attenuation and 50 shots. Each experiment was repeated at least 5 times, and the averaged data were collected.

Pro-Peptide Labeling with Dansyl Chloride. Labeling of the wild-type or mutant (D9A) pro-peptide was performed as described (*37*), with few modifications. Briefly, wild-type or mutant pro-peptide was dissolved in 0.1 M sodium bicarbonate, pH 8.6, to a final concentration of 10 mg/mL. The peptide solution was mixed while vortexing with 0.1 volume of 10 mg/mL dansyl chloride in DMF, followed by incubation overnight at 4 °C on a rotative wheel. The labeled peptide was separated from unreacted reagent using a Sephadex G-15 column (1 × 18 cm), equilibrated with 50 mM potassium phosphate, pH 7.5. The flow-through, containing the conjugated pro-peptide, was stored at −20 °C. The degree of labeling was determined by calculating the concentration of dansyl chloride conjugate (ϵ_{345} = 3400 M^{-1} cm^{-1}) and by comparison to the initial concentration of pro-peptide. The degrees of labeling of mutant pro-peptide and wild-type pro-peptide were 50% and 40%, respectively.

RESULTS

Comparison of Procaspase-3(C163S) and the Pro-less Variant. Procaspase-3 consists of 277 amino acids, with a M_r of 32 642 (including the LEH_6 sequence used for purification). Although under normal conditions in human cells the protein does not autoprocess, it has been shown to autoprocess under conditions in which the protein is over-expressed or the pro-domain is removed (*7*, *24*). To examine the oligomeric and spectroscopic properties of procaspase-3 without the complicating autoprocessing reactions, we mutated the active site cysteinyl residue to serine. Mutations of Cys163 have been shown to abrogate activity, but are not structurally perturbing (*19*, *38*−*40*). To examine the structure of the pro-domain within the procaspase, we constructed a mutant of procaspase-3(C163S), called the pro-less variant, in which the pro-peptide was removed by cloning (M_r = 29 658). In this protein, the amino terminus begins with a methionine residue, which is absent from processed protease purified from cells. The amino terminus of protease purified from human cells begins with Ser29. Both procaspase-3(C163S) and the pro-less variant were analyzed by MALDI-TOF mass spectrometry to confirm the correct mass (data not shown).

Procaspase-3 and the Pro-less Variant Are Dimers. To examine the oligomeric properties of procaspase-3 and the pro-less variant, we initially examined their elution profiles by size exclusion chromatography using Sephacryl S-100 HR resin at room temperature (data not shown). Results from these experiments showed that procaspase-3(C163S) eluted with an apparent molecular weight of 64 773, approximately equal to the mass of a dimer (for the monomer, $M_r = 32\,642$). Likewise, the pro-less variant eluted with an apparent molecular weight of 59 106 (for the monomer, $M_r = 29\,658$). There were no additional peaks corresponding to the monomer molecular weight, suggesting that at the protein concentrations of these experiments, 10 μM, both procaspase-3(C163S) and the pro-less variant are dimers.

To confirm that both proteins are dimers, we used sedimentation equilibrium to examine their oligomeric properties. The proteins were examined over a wide range of protein concentrations and at several rotor speeds (see Materials and Methods). Representative data are shown in Figure 2, panels A [procaspase-3(C163S)] and C (pro-less variant).

For both proteins, the data were best fit to a single, thermodynamically ideal species that corresponds to a dimer. The average molecular weights determined from the fits of all data sets were 65 573 for procaspase-3(C163S) and 58 342 for the pro-less variant. The residuals to the fits for both proteins (Figure 2, panels B and D) demonstrate that the data are well fit to the model.

In these experiments, there was no evidence for formation of a monomeric species, even at the lowest protein concentration (~450 nM) of the experiment. An accurate determination of the equilibrium dissociation constant is not possible under these conditions because we were unable to populate the monomeric species at the lowest protein concentration, which was at the detection limit of the instrument when the absorbance at 230 nm was monitored. However, if we assume a simple model for dissociation of a dimer to two monomers, and given the fact that the proteins are dimers at protein concentrations of 450 nM, we can estimate the upper limit for the equilibrium dissociation constant of the dimer to the monomer to be 50 nM, although it may be much lower.

Secondary and Tertiary Structural Properties of Procaspase-3 Do Not Change Significantly after Pro-Domain Removal. Procaspase-3 has 2 tryptophans in the C-terminal region (Trp206 and Trp214), as well as several tyrosines (10) and phenylalanines (15) that are well-dispersed throughout the sequence. Although the structure of the procaspase is not known, in the mature heterotetramer the two tryptophans are in close contact. Tryptophan 206 forms part of the S2 binding pocket (*7*), whereas tryptophan 214 is found in the S4 site and hydrogen bonds to the substrate. There are no aromatic amino acids in the pro-domain of procaspase-3. These features allow for the study of potential changes in the fluorescence emission of the procaspase-3 dimer upon removal of the pro-domain by monitoring fluorescence emission between 300 and 400 nm following excitation either at 280 nm, to excite all aromatic amino acids, or at 295 nm, to excite primarily the tryptophanyl residues.

As shown in Figure 3, panel A, the fluorescence emission spectra following excitation at 280 nm are superimposable for procaspase-3(C163S) and the pro-less variant. Both proteins demonstrate an emission maximum at 335 nm. The

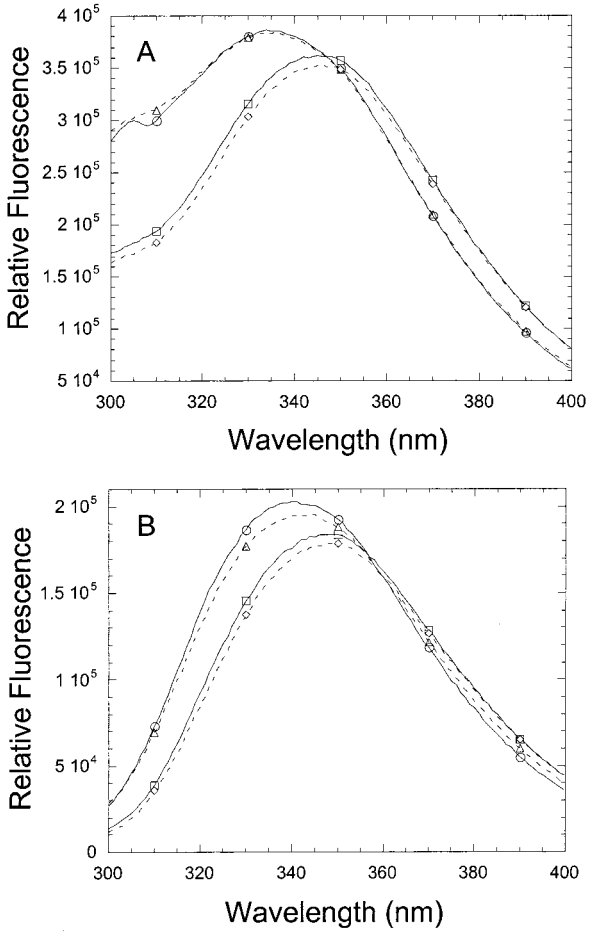

FIGURE 3: Fluorescence emission spectra of native and unfolded procaspase-3(C163S) and pro-less variant. Proteins (1 μM) were in 50 mM KH_2PO_4/K_2HPO_4, pH 7.2, 1 mM DTT, 25 °C, with or without 8 M urea. The samples were excited at 280 nm (panel A) or 295 nm (panel B), and the fluorescence emission was collected from 300 to 400 nm. For panels A and B: (○) native procaspase-3(C163S); (△) native pro-less variant; (□) unfolded procaspase-3(C163S); (◇) unfolded pro-less variant.

fluorescence emission following excitation at 295 nm shows similar results (Figure 3, panel B). In this case, the emission maximum for procaspase-3(C163S) is 340 nm, whereas that for the pro-less variant is slightly red-shifted to 341 nm. In addition, the fluorescence emission of the pro-less variant is quenched slightly (~2%). Following unfolding in 8 M urea, the emission maxima are red-shifted to 346 nm (Figure 3, panel A) or 348 nm (Figure 3, panel B), and the fluorescence emission decreases by ~10%. These results are consistent with our equilibrium unfolding data (see preceding paper, *62*), which show that procaspase-3(C163S) is largely unfolded under these conditions.

We compared the secondary and tertiary structures of procaspase-3(C163S) and the pro-less variant by monitoring near- and far-UV circular dichroism, and the data are shown in Figure 4. In the far-UV, procaspase-3(C163S) demonstrates two minima (208 and 215 nm) (Figure 4, spectrum 1), although the amplitudes of the minima are very similar. While it is not possible to deconvolute these data into their component secondary structural elements due to the limitations of our instrument, based on reference spectra described by Johnson (*41*), the data are consistent with a protein that contains both α-helix and β-sheet elements, with the α-heli-

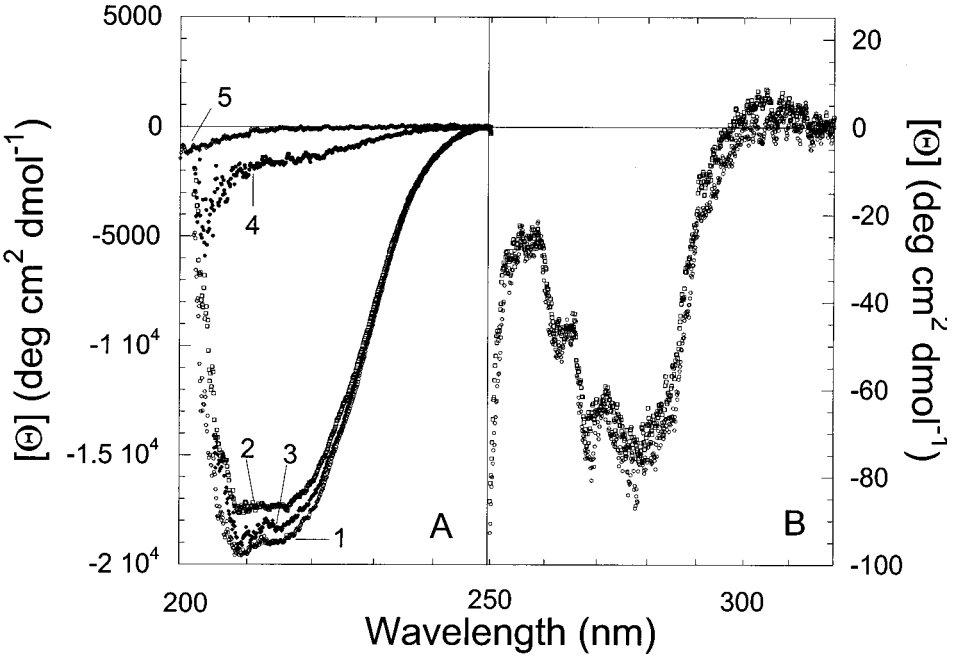

FIGURE 4: Near- and far-UV circular dichroism spectra of procaspase-3(C163S), pro-less variant, and pro-peptide. The experiments were performed at 25 °C in a buffer containing 20 mM KH_2PO_4/K_2HPO_4, pH 7.2, 0.1 mM DTT. Protein concentrations were 20 μM. (Panel A) Far-UV CD spectra: (1) procaspase-3(C163S); (2) pro-less variant; (3) pro-less variant with pro-peptide in trans; (4) procaspase-3(C163S) minus pro-less variant (spectrum 1 minus spectrum 2); (5) pro-peptide. (Panel B) Near-UV CD spectra: (○) procaspase-3(C163S); (□) pro-less variant.

cal structures contributing to the minimum at 208 nm. The far-UV CD spectrum for the pro-less variant (Figure 4, spectrum 2) is similar to that of procaspase-3 except that the minimum at 208 nm is less pronounced. In addition, there is a decrease in amplitude of approximately 10% between the pro-less variant and procaspase-3(C163S), consistent with the loss of about 10% of the total number of amino acids in the pro-less variant (28 amino acids from 285 amino acids). The spectra are superimposable when the data (spectra 1 and 2 in Figure 4) are normalized by the total number of amino acids in each protein, that is, the mean residue ellipticity (data not shown). This suggested that the secondary structure of the procaspase-3(C163S) dimer was unaffected by the loss of the pro-domain.

The near-UV CD spectra (Figure 4) for procaspase-3 and the pro-less variant are superimposable. The data demonstrate minima at 280 and 270 nm as well as a maximum at 255 nm, indicative of well-packed tertiary structures. The fluorescence emission data shown in Figure 3, panel B, suggested that there might be a conformational change in the protein due to loss of the pro-domain. However, results from circular dichroism (Figure 4) suggest that the structural changes may be localized to the environment of the two tryptophan residues in the pro-less variant. While it is not yet clear whether the localized structural changes affect protein stability, there is no effect on dimerization (Figure 2).

The Structure of the Pro-Domain Bound to the Procaspase Dimer Is Different than the Pro-Domain in Solution. A comparison of the far-UV CD spectra (Figure 4) for procaspase-3(C163S) and the pro-less variant suggested that the pro-domain may contain secondary structural elements that contribute to the spectrum of the full-length protein. We have subtracted the two spectra (Figure 4, spectra 1 and 2), and the results are shown in Figure 4 (spectrum 4). Because the mean residue ellipticity spectra are superimposable for the two proteins (data not shown), conformational changes, if any, in the protein as a result of removal of the pro-domain do not affect the far-UV spectral properties. Therefore, we suggest that spectrum 4 in Figure 4 represents the pro-domain of procaspase-3. We have examined the pro-domain (28 amino acids) under the same solution conditions as those described for procaspase-3 (Figure 4) in order to compare the far-UV CD properties of the pro-domain with those of the subtracted spectra. The far-UV CD spectrum for the pro-domain in solution is shown as spectrum 5 in Figure 4. In the absence of the protease domain, the pro-peptide appears to contain primarily random structure. We also examined the CD spectra at several concentrations of pro-peptide (10−100 μM) and found no change in the CD spectra with an increase in protein concentration (data not shown). These results demonstrated that the pro-domain does not self-associate under the conditions of these experiments. In support of this, we examined the peptide by native gel electrophoresis (data not shown) at concentrations of ~500 μM and observed only a monomeric peptide. Together, these results demonstrate that the pro-domain of procaspase-3 does not self-associate and suggest that it contains secondary structure when present in cis to the remaining protease domain.

FTIR Spectra Suggest the Pro-Domain Is a β-Strand. To examine the interactions of the pro-domain with the pro-less variant, especially the structure of the pro-domain, we examined procaspase-3(C163S), the pro-less variant, and the pro-peptide by FTIR, and the results are shown in Figure 5. While the details are described elsewhere (*42*), a method was developed for collecting FTIR spectra using attenuated total reflection spectroscopy in a Fourier transform infrared microscope that presents an extremely rapid and sensitive means of determining the amide I line shape in H_2O.

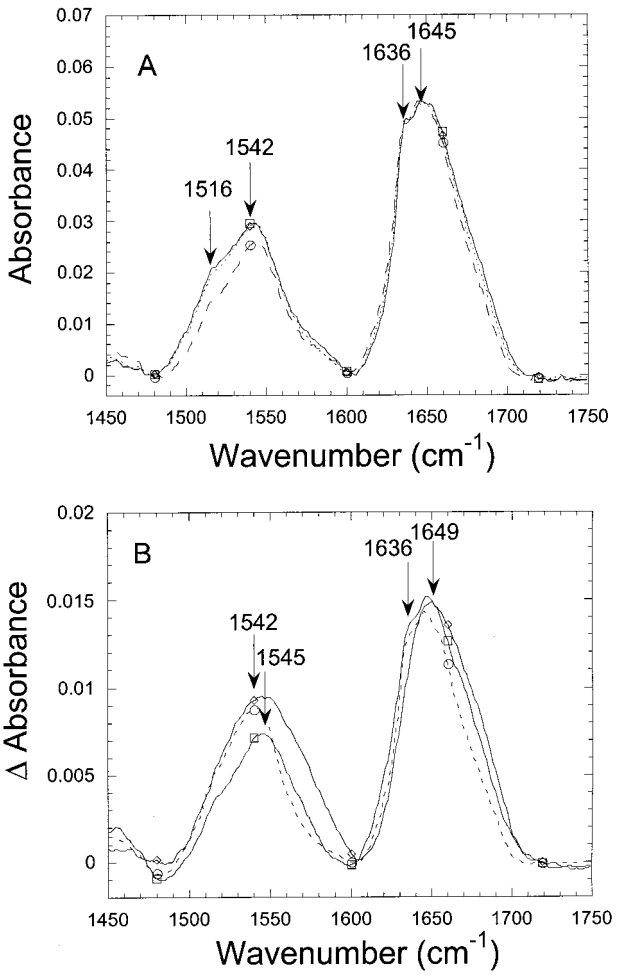

FIGURE 5: FTIR spectra of procaspase-3(C163S), pro-less variant, and pro-peptide. (Panel A) FTIR spectra for procaspase-3(C163S) (□), pro-less variant (◇), and a mixture of pro-less variant with pro-peptide (○). (Panel B) FTIR spectra of pro-peptide (◇), procaspase-3(C163S) minus pro-less variant (○), and pro-less variant in a mixture with pro-peptide minus the spectrum of the pro-less variant (□).

Representative spectra for procaspase-3(C163S) and the pro-less variant are shown in Figure 5, panel A. The data demonstrate similar spectral shapes for both proteins in the amide I region with peaks at 1636 and 1645 cm^{-1}. In addition, both proteins have peaks in the amide II region at 1542 and 1516 cm^{-1}. These spectra are consistent with an α/β protein (*42*). Consistent with the fluorescence and CD spectra (Figures 3 and 4), the FTIR spectra demonstrate that removal of the pro-peptide has little effect on the remainder of the procaspase-3 dimer.

As described for the circular dichroism spectra in Figure 4, the FTIR spectra shown in Figure 5A were subtracted in order to obtain the contribution of the pro-domain to the spectrum, and the data were compared to the pro-peptide free in solution. The results are shown in Figure 5, panel B. The spectrum of the pro-peptide in solution (Figure 5B, diamonds) shows a single peak at 1649 cm^{-1} in the amide I region as well as a peak at 1545 cm^{-1} in the amide II region. In comparison, the subtracted spectrum (procaspase-3 minus pro-less variant) (Figure 5B, circles) demonstrates peaks at 1645 and 1636 cm^{-1} in the amide I region as well as a peak at 1542 cm^{-1} in the amide II region. The correlations between protein structure and amide I bands are well-known (*42*) and indicate that the pro-peptide, in solution, is a random coil, whereas the pro-peptide in cis to the protease domain (that is, in procaspase-3) contains β-structure. Currently, we cannot interpret the shifts in the amide II region because there are no correlations as for the amide I band. When these spectra are interpreted with the results from circular dichroism (Figure 4), the data suggest that the pro-domain of procaspase-3 is not a random coil when in cis to the protease domain, but rather may be a β-strand that forms hydrogen bonds with the protease domain. The pro-peptide free in solution, however, appears to be a random coil.

The Pro-Domain Interacts with the Pro-less Variant in Trans. The pro-less variant was incubated with the pro-domain in trans in order to determine whether the pro-peptide interacts with the protease domain when not covalently attached to the protease domain. As shown in Figure 4 (spectrum 3), a mixture of pro-less variant with the pro-domain (20 μM of each) resulted in an increase in ellipticity at 208 nm and at 215 nm. Compared to the spectrum of procaspase-3 (Figure 4, spectrum 1), approximately 70% of the ellipticity was obtained. No further increase occurred when the pro-domain was in excess of the pro-less variant (data not shown). In addition, the near-UV CD spectra (data not shown) were identical to those shown in Figure 4. These results suggest that the pro-domain interacts with the pro-less variant and adopts a structure similar to the pro-domain in full-length procaspase-3. Formally, it remains possible that the differences in CD spectra are due to conformational changes in the pro-less variant. While we cannot rule out this possibility, the data demonstrate that the pro-peptide interacts with the protease domain in trans. It seems unlikely that the structure of the pro-peptide would remain a random coil when bound to the protease domain.

The mixture of pro-less variant plus pro-domain was also analyzed by FTIR. As shown in Figure 5, panel A, the spectrum for the mixture was superimposable with that of full-length procaspase-3(C163S) in the amide I region. This does not occur simply by adding the individual spectra (data not shown), indicating that structure is induced in the pro-domain while in the presence of the pro-less variant. The spectrum for the pro-less variant was subtracted from that for the mixture (pro-less variant plus pro-peptide), and the results are shown in Figure 5, panel B (squares). The resulting spectrum is intermediate with those for the peptide in solution (Figure 5B, diamonds) and the pro-peptide in cis to the protease domain (Figure 5B, circles). For example, the peptide in trans has two peaks in the amide I region at 1647 and 1636 cm^{-1}, similar to the pro-peptide in cis. However, the peak in the amide II region is similar to that for the pro-peptide in solution. These spectra are consistent with both β-sheet and random coil components to the pro-peptide when it is in the presence of the protease domain, which may be due to weak binding of the pro-peptide to the pro-less variant.

To confirm the interactions of the pro-peptide with the pro-less variant, we measured the changes in fluorescence anisotropy of a pro-peptide labeled with dansyl chloride as it was titrated with the pro-less variant. The data are shown in Figure 6. In these experiments, either the dansylated wild-type pro-peptide (Figure 6, squares) or the D9A mutant pro-peptide (Figure 6, circles) was titrated with the pro-less variant. The data show that both pro-peptides bind to the

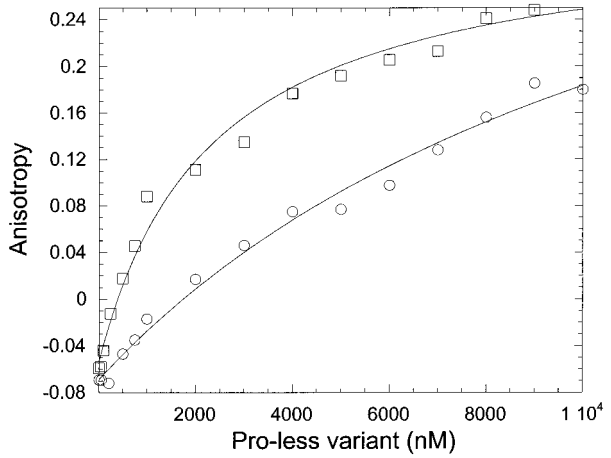

FIGURE 6: Fluorescence anisotropy of pro-peptide in the presence of pro-less variant. The dansyl-labeled wild-type pro-peptide (□) or the dansyl-labeled D9A mutant pro-peptide (○) (1 μM) was titrated with the pro-less variant. All assays were carried out at 25 °C in a buffer of 50 mM potassium phosphate, pH 7.5, 1 mM DTT. The solid lines represent fits of the data to a simple binding model, as described under Materials and Methods.

pro-less variant, although the wild-type pro-peptide appears to bind more tightly than the D9A mutant peptide. While the interactions may be more complex, we assumed a simple binding model to describe the interactions (solid lines in Figure 6). Overall, the data demonstrate the pro-peptides bind to the pro-less variant with equilibrium dissociation constants in the low micromolar range and confirm the interactions observed by circular dichroism (Figure 4) and FTIR (Figure 5).

Pro-domain Is neither a Good Substrate nor a Good Inhibitor of Caspase-3. Because of the spectroscopic data described above, we examined the activity of the mature caspase-3 protease in the presence of the pro-peptide in order to examine interactions with the protease domain in trans. The results of these studies are shown in Figure 7. The data in Figure 7, panel A, show the enzyme activity of caspase-3 in the presence of a fluorescence substrate (DEVD-AFC) and with increasing amounts of the irreversible caspase inhibitor Z-VAD-FMK. The data demonstrate a decrease in activity with an increase in inhibitor concentration. As shown previously (*26*), the data are well-described by eq 1, and the second-order rate constant for binding of inhibitor to caspase-3 (described under Materials and Methods) is in agreement with that determined previously (*6*), $\sim 3 \times 10^3$ M^{-1} s^{-1}. In contrast to the caspase inhibitor, there was no change in enzyme activity in the presence of the pro-peptide, as shown in Figure 7, panel B. In these studies, the concentration of the pro-peptide was varied (from 0 to 500 μM), and there was no change in activity. In agreement with previous reports (*14*), these results show that the pro-peptide does not inhibit the activity of the caspase-3 protease.

While the enzymatic data (Figure 7, panel A) indicated that the pro-domain does not inhibit the protease, it is possible that the pro-peptide may be a substrate of the caspase-3 protease. Simulations of the enzymatic reactions (data not shown) using the program Kinsim (*43*) demonstrate that production of AFC product from the DEVD-AFC substrate would be unaffected so long as the binding of the pro-peptide were weaker than that of the fluorescent substrate

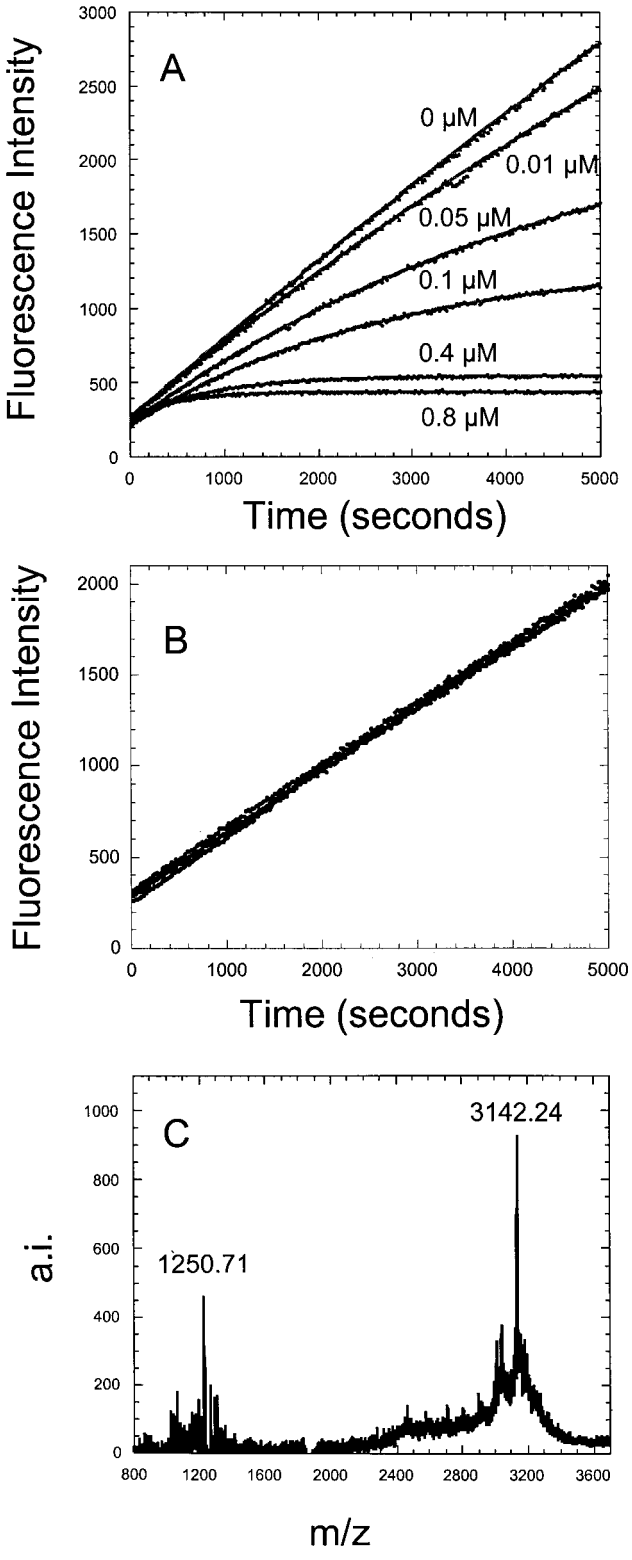

FIGURE 7: Pro-domain influence on caspase-3 activity. Caspase-3 (0.1 nM) and DEVD-AFC substrate (10 μM) were incubated in assay buffer in the presence of inhibitor or pro-peptide as described under Materials and Methods. Fluorescence emission of generated AFC was monitored at 505 nm after excitation at 400 nm. (Panel A) Caspase-3 assay in the presence of the inhibitor Z-VAD-FMK. The inhibitor concentrations are indicated. (Panel B) Caspase-3 assay in the presence of wild-type and mutant (D9A) pro-peptide (0−500 μM). (Panel C) MALDI-TOF analysis of caspase-3 reaction products after hydrolysis of wild-type or mutant (D9A) pro-domain by caspase-3. The peak at 3142 Da represents the full-length pro-peptide.

(DEVD-AFC) and the binding of the pro-peptide were reversible. Based on the structure described recently (*44*) of the procaspase-3 maturation intermediate bound to an inhibitor, XIAP, both of these criteria seem likely. In that structure, the pro-peptide is disordered in the crystal.

We examined whether the pro-peptide is a substrate for caspase-3 in two ways. First, we tested the enzyme activity of the caspase-3 protease in the presence of a mutant of the pro-peptide in which Asp9 was replaced with alanine ($NSVA^9$). This peptide would not be cleaved by the protease. As shown in Figure 7, panel B, there was no change in the enzyme activity in the presence of up to 500 μM pro-peptide, confirming that the pro-peptide does not inhibit activity. In separate experiments, the enzyme concentration was 0.1, 1, or 10 nM, and the results were the same as those shown in Figure 7B. Second, in separate reactions, we incubated the pro-peptide (wild-type or D9A mutant) with active caspase-3 enzyme under conditions similar to those in Figure 7 except that the substrate (DEVD-AFC) was not added. We then examined the products, if any, of the enzymatic reaction by SDS−PAGE and MALDI-TOF mass spectrometry. If cleavage occurred at Asp9 in the wild-type pro-peptide, then the molecular weight would decrease from one species of ~3130 to two species of ~1030 and ~2100. The SDS−PAGE analysis of the enzymatic reactions showed a single species for the wild-type pro-peptide as well as for the D9A mutant pro-peptide (data not shown). Results from the MALDI-TOF analysis are shown in Figure 7C. For both the wild-type and mutant pro-peptides, only a single species was observed with M_r ~3100. In Figure 7C, the peak at M_r 1250 arises from the buffer, as determined from control experiments of buffer alone (data not shown). These data suggest that while the pro-domain does not inhibit the activity of caspase-3, it is not a good substrate when in trans to the mature protease.

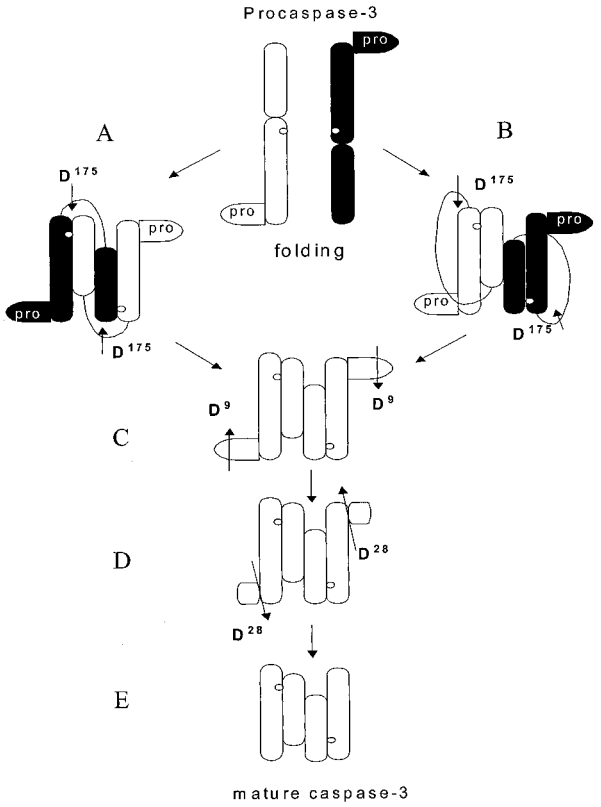

FIGURE 8: Model for procaspase-3 assembly and maturation. Before processing, two molecules of procaspase-3 form a dimer by interdigitation (structure A) or association (structure B), generating a structure similar to the one of caspase-3 heterotetramer. The dimeric procaspase is cleaved at Asp175 to form the maturation intermediate (structure C). The pro-domain is then cleaved rapidly at Asp9 (structure D), then more slowly at Asp28 to give the mature heterotetramer (structure E). The catalytic site is schematized as a white ball.

DISCUSSION

We have shown that human procaspase-3 is a dimer in solution, and we estimate the upper limit for the equilibrium dissociation constant to be ~50 nM. Removal of the pro-peptide has little effect on the equilibrium dissociation constant of the dimer or on the spectroscopic properties of the dimer, indicating that the dimeric structure is likely to be unaltered in the pro-less mutant. Results from circular dichroism, fluorescence anisotropy, and FTIR studies suggest that the pro-peptide interacts weakly with the dimer. In addition, the data suggest that the pro-peptide adopts a β-structure when in contact with the protein, either covalently attached (in cis), as for the procaspase-3, or when added in trans, as for the pro-less variant. Surprisingly, while the pro-peptide does not inhibit the activity of the mature caspase-3 heterotetramer, our data suggest that the pro-peptide is a poor substrate for the enzyme.

The question remains, however, whether the procaspase dimer observed in vitro is relevant to the oligomeric state of the protein in vivo. First, our folding data (*62*) demonstrate that dimerization of procaspase-3(C163S) occurs through a folding intermediate rather than through the native, monomeric procaspase-3, demonstrating that dimerization is a folding event. Second, based on the average volume of a Jurkat T cell, ~9.5×10^{-10} mL (*45*), and the quantity of caspase-3 heterotetramer in apoptotic Jurkat cells (6.6 ng/10^6 cells) (*46*), we estimate the concentration in vivo of the active caspase-3 to be ~100 nM. Salvesen and co-workers have quantified caspase-3 in 293 cells and found the same concentration (~100 nM) (*14*). In the case of caspase-1, the concentration of the procaspase has been shown to be >10-fold higher than the activated form (*47*, *48*). If this is true for caspase-3, then the concentrations of procaspase-3 may be much higher than 100 nM. Third, Cohen and co-workers (*49*, *50*) demonstrated that procaspase-3 from THP.1 cell lysates eluted as a dimer from a gel filtration column. This occurred in both control (nonapoptotic) and apoptotic cells (*49*). Together, the data strongly suggest that procaspase-3 is a dimer in vivo.

These results are important because they suggest that dimerization is an early event in procaspase-3 maturation, similar to that described for procaspase-1 and activator procaspases (*40*). Our results as well as previous studies (*51*) suggest the model shown in Figure 8 for maturation of procaspase-3. In this model, dimeric procaspase is the result of either interdigitation or association of two precursors. In the first case, large and small subunits from different molecules contribute to the catalytic center, whereas in the latter case this is preformed within the same monomer. In both cases, the interface is generated predominantly by interactions between the small subunits, as in mature caspase-3. The dimeric procaspase-3 is cleaved at Asp175 to separate the covalent linkage of the large and small subunits. The

pro-peptide is then cleaved rapidly at Asp9, then more slowly at Asp28, generating the mature heterotetramer. This model is consistent with the recent crystal structure of the procaspase-3 maturation intermediate with the inhibitor XIAP bound, which shows that the intermediate of maturation is a dimer with inhibitor bound to each active site (*44*). While it is not known whether the dimeric procaspase structure involves a domain-swap as shown in the Figure 8, this was suggested from the crystal structures of the mature heterotetramer (*6*, *7*) based on the positions of the C-terminal ends of the large subunits and the N-terminal ends of the small subunits. In the case of procaspase-1 (*40*), both intercalated and nonintercalated structures have been shown to form. Whether the procaspase-3 dimer results from domain-swapping remains to be determined, although one should note that following cleavage at Asp175, the maturation intermediate from either form of the procaspase would be indistinguishable, as shown in Figure 8.

The question remains why the procaspase-3 dimer is inactive in vivo such that autocatalytic processing does not occur. We suggest two reasons for this. First, rather than the canonical caspase-3 recognition sequence (DEVD), the tetrapeptide sequence at Asp175 ($IETD^{175}$) is optimal for caspases in subclass III, caspases-6, -8, -9, all of which activate procaspase-3 (*52*). Thornberry and co-workers (*53*) and Salvesen and co-workers (*54*) have shown that substitutions at the P4 position of the substrate have a dramatic effect on the ability of caspase-3 to cleave the substrate. In some cases, the caspase-3 activity is only a small fraction when compared to that for the optimal sequence. Second, the low activity is coupled to low protein concentrations (~100 nM). Increasing either of these two factors (activity or concentration) would lead to autoactivation. In the case of protein expressed from heterologous expression systems, the procaspase-3 dimer autoactivates because of the high protein concentrations. Although we have shown that the pro-peptide is not a good substrate for caspase-3 in trans, the locally high concentrations when it is present in cis to the protease domain allows for cleavage of the pro-peptide. Therefore, an increase in activity, as observed in the maturation intermediate, could lead to cleavage of the pro-peptide. The active intermediate or mature enzyme would feed back to activate procaspase-3.

Pro-domains from many protease zymogens have been shown to interact with the protease domain either to inhibit activity (*55*) or to influence folding as an intramolecular chaperone (*56*, *57*). In those systems, the pro-domains are generally much larger than that for procaspase-3. Recently, however, the pro-peptide of β-secretase, which consists of 24 amino acids, was shown to increase the yield of correctly folded protein when present in cis or in trans (*58*). Although the nature of the interactions is not yet known, we have shown that the caspase-3 pro-peptide interacts weakly with the protease domain of the zymogen. In contrast with long pro-domain caspases, procaspase-3 does not utilize its pro-domain in dimerization, because the pro-less variant described here is also a dimer. Most probably, procaspase-3 forms dimers using the same residues involved in the mature caspase-3 heterodimer−heterodimer interface. The nature of this interface, with Val266−Val266# at the 2-fold symmetry axis, suggests that the driving force in procaspase-3 dimerization is based on hydrophobic interactions. This is not the case for caspases-1, -4, and -5, where the interface between the small subunits contains two salt-bridges. In those caspases, the CARD−CARD interactions between the pro-domains and adapter proteins apparently precede other contacts, but are not sufficient to keep the dimer in a stable conformation (*19*, *59*).

The possibility remains that the pro-peptide of procaspase-3 may act to attenuate the low levels of activity of the procaspase dimer, which would further serve as a control over activation. Alternatively, in comparison with subtilisin (*60*), for example, the pro-peptide may function as an intramolecular chaperone to assist in procaspase-3 folding. Either of these possibilities would suggest that pro-domains from the activator caspases, which contain the CARD motifs, are bifunctional. The remaining possibility is that the pro-peptides of the executioner caspases are simply vestigial linkers that connect the CARD motif to the amino terminus of the large subunit. Because the executioner caspases are activated by other caspases in the cascade, the CARD motif may have been lost through evolution, whereas the linker was retained. Further experiments will determine the role of the procaspase pro-peptide among these intriguing possibilities.

ACKNOWLEDGMENT

We thank Luming He and Randy Durren for their technical expertise. We also thank Dr. Dennis Brown for use of the HPLC. We are grateful to Dr. Emad Alnemri for supplying procaspase-3 cDNA and to Dr. Jim Hu for helpful discussions and for use of the analytical ultracentrifuge, allowing us to perform initial experiments.

REFERENCES

1. Earnshaw, W. C., Martins, L. M., and Kaufmann, S. H. (1999) *Annu. Rev. Biochem. 68*, 383−424.
2. Marks, N., and Berg, M. J. (1999) *Neurochem. Int. 35*, 195−220.
3. Wolf, B. B., and Green, D. R. (1999) *J. Biol. Chem. 274*, 20049−20052.
4. Tewari, M., Quan, L. T., O'Rouke, K., Desnoyers, S., Zeng, Z., Beidler, D. R., Poirier, G. G., Salvesen, G. S., and Dixit, V. M. (1995) *Cell 81*, 801−809.
5. Kuida, K., Zheng, T. S., Na, S., Kuan, C.-Y., Yang, D., Karasuyama, H., Rakic, P., and Flavell, R. A. (1996) *Nature 384*, 368−372.
6. Rotonda, J., Nicholson, D. W., Fazil, K. M., Gallant, M., Gareau, Y., Labelle, M., Peterson, E. P., Rasper, D. M., Ruel, R., Vaillancourt, J. P., Thornberry, N. A., and Becker, J. W. (1996) *Nat. Struct. Biol. 3*, 619−625.
7. Mittl, P. R. E., DiMarco, S., Krebs, J. F., Bai, X., Karanewsky, D. S., Priestle, J. P., Tomaselli, K. J., and Grutter, M. G. (1997) *J. Biol. Chem. 272*, 6539−6547.
8. Thornberry, N. A., Bull, H. G., Calaycay, J. R., Chapman, K. T., Howard, A. D., Kostura, M. J., Miller, D. K., Molineaux, S. M., Weidner, J. R., Aunins, J., Elliston, K. O., Ayala, J. M., Casano, F. J., Chin, J., Ding, G. J.-F., Egger, L. A., Gaffney, E. P., Limjuco, G., Palyha, O. C., Raju, S. M., Rolando, A. M., Salley, J. P., Yamin, T.-T., Lee, T. D., Shively, J. E., MacCross, M., Mumford, R. A., Schmidt, J. A., and Tocci, M. J. (1992) *Nature 356*, 768−774.
9. Walker, N. P. C., Talanian, R. V., Brady, K. D., Dang, L. C., Bump, N. J., Ferenz, C. R., Franklin, S., Ghayur, T., Hackett, M. C., Hammill, L. D., Herzog, L., Hugunin, M., Houy, W., Mankovich, J. A., McGuiness, L., Orlewicz, E., Paskind, M., Pratt, C. A., Reis, P., Summani, A., Terranova, M., Welch, J. P., Xiong, L., Moller, A., Tracey, D. E., Kamen, R., and Wong, W. W. (1994) *Cell 78*, 343−352.

10. Watt, W., Koeplinger, K. A., Mildner, A. M., Heinrikson, R. L., Tomasselli, A. G., and Watenpaugh, K. D. (1999) *Structure 7*, 1135−1143.
11. Chai, J., Shiozaki, E., Srinivasula, S. M., Wu, Q., Dataa, P., Alnemri, E. S., and Shi, Y. (2001) *Cell 104*, 769−780.
12. Yamin, T.-T., Ayala, J. M., and Miller, D. K. (1996) *J. Biol. Chem. 271*, 13273−13282.
13. Han, Z., Hendrickson, E. A., Bremner, T. A., and Wyche, J. H. (1997) *J. Biol. Chem. 272*, 13432−13436.
14. Stennicke, H. R., Jurgensmeier, J. M., Shin, H., Deveraux, Q., Wolf, B. B., Yang, X., Zhou, Q., Ellerby, M., Ellerby, L. M., Bredesen, D., Green, D. R., Reed, J. C., Froelich, C. J., and Salvesen, G. S. (1998) *J. Biol. Chem. 273*, 27084−27090.
15. Mancini, M., Nicholson, D. W., Roy, S., Thornberry, N. A., Peterson, E. P., Casciola-Rosen, L. A., and Rosen, A. (1998) *J. Biol. Chem. 140*, 1485−1495.
16. Shin, S., Sung, B.-J., Cho, Y.-S., Kim, H.-J., Ha, N.-C., Hwang, J.-I., Chung, C.-W., Jung, Y.-K., and Oh, B.-H. (2001) *Biochemistry 40*, 1117−1123.
17. Cohen, G. (1997) *Biochem. J. 326*, 1−16.
18. Chou, J., Matsuo, H., Duan, H., and Wagner, G. (1998) *Cell 94*, 171−180.
19. Van Criekinge, W., Beyaert, R., Van de Craen, M., Vandenabeele, P., Schotte, P., De Valck, D., and Fiers, W. (1996) *J. Biol. Chem. 271*, 27245−27248.
20. Stennicke, H. R., and Salvesen, G. S. (1998) *Biochim. Biophys. Acta 1387*, 17−31.
21. Ryser, S., Vial, E., Magnenat, E., Schlegel, W., and Maundrell, K. (1999) *Curr. Genet. 36*, 21−28.
22. Fernandes-Alnemri, T., Litwack, G., and Alnemri, E. S. (1994) *J. Biol. Chem. 269*, 30761−30764.
23. Dorstyn, L., Kinoshita, M., and Kumar, S. (1998) *Results Probl. Cell Differ. 24*, 1−24.
24. Meergans, T., Hildebrandt, A.-K., Horak, D., Haenisch, C., and Wendel, A. (2000) *Biochem. J. 349*, 135−140.
25. Fernandes-Alnemri, T., Litwack, G., and Alnemri, E. S. (1995) *Cancer Res. 55*, 2737−2742.
26. Stennicke, H. R., and Salvesen, G. S. (1999) *Methods 17*, 313−319.
27. Laemmli, U. K. (1970) *Nature 227*, 680−685.
28. Clark, A. C., Ramanathan, R., and Frieden, C. (1998) *Methods Enzymol. 290*, 100−118.
29. Edelhoch, H. (1967) *Biochemistry 6*, 1948−1954.
30. Stennicke, H. R., and Salvesen, G. S. (1997) *J. Biol. Chem. 272*, 25719−25723.
31. Zhou, Q., Krebs, J. F., Snipas, S. J., Price, A., Alnemri, E. S., Tomaselli, K. J., and Salvesen, G. S. (1998) *Biochemistry 37*, 10757−10765.
32. Hedegs, J., Sarrafzadeh, S., Lear, J. D., and McRorie, D. K. (1984) *Modern Analytical Ultracentrifugation* (Schuster, T. M., and Laue, T. M., Eds.) Birkhäuser, Boston, MA.
33. Johnson, M., Correa, I., Yphantis, D., and Halvorson, H. (1981) *Biophys. J. 36*, 575−588.
34. Lakowicz, J. R. (1983) *Principles of fluorescence spectroscopy* (Orton, C. G., Ed.) Plenum Press, New York.
35. Connolly, K. M., Ilangovan, U., Wojciak, J. M., Iwahara, M., and Clubb, R. T. (2000) *J. Mol. Biol. 300*, 841−856.
36. Morrison, J. F., and Walsh, C. T. (1998) *Adv. Enzymol. Relat. Areas Mol. Biol. 59*, 201−301.
37. Haugland, R. (1995) *Methods Mol. Biol. 45*, 205−221.
38. Colussi, P. A., Harvey, N. L., Shearwin-Whyatt, L. M., and Kumar, S. (1998) *J. Biol. Chem. 1998*, 26566−26570.
39. Stennicke, H. R., Deveraux, Q. L., Humke, E. W., Reed, J. C., Dixit, V. M., and Salvesen, G. S. (1999) *J. Biol. Chem. 274*, 8359−8362.
40. Gu, Y., Wu, J., Faucheu, C., Lalanne, J.-L., Diu, A., Livingston, D. J., and Su, M. S.-S. (1995) *EMBO J. 14*, 1923−1931.
41. Johnson, W. C., Jr. (1990) *Proteins: Struct., Funct., Genet. 7*, 205−214.
42. Jackson, M., and Mantsch, H. H. (1995) *Crit. Rev. Biochem. Mol. Biol. 30*, 95−120.
43. Barshop, B. A., Wrenn, R. F., and Frieden, C. (1983) *Anal. Biochem. 130*, 134−145.
44. Riedl, S. J., Renatus, M., Schwarzenbacher, R., Zhou, Q., Sun, C., Fesik, S. W., Liddington, R. C., and Salvesen, G. S. (2001) *Cell 104*, 791−800.
45. Ivanov, I. B., Hadjiiski, A., Denkov, N. D., Gurkov, T. D., Kralchevsky, P. A., and Koyasu, S. (1998) *Biophys. J. 75*, 545−556.
46. Saunders, P. A., Cooper, J. A., Roodell, M. M., Schroeder, D. A., Borchert, C. J., Isaacson, A. L., Schendel, M. J., Godfrey, K. G., Cahill, D. R., Walz, A. M., Loegering, R. T., Gaylor, H., Woyno, I. J., Kaluyzhny, A. E., Krzyzek, R. A., Mortari, F., Tsang, M., and Roff, C. F. (2000) *Anal. Biochem. 284*, 114−124.
47. Ayala, J. M., Yamin, T.-T., Egger, L. A., Chin, J., Kostura, M., and Miller, D. K. (1994) *J. Immunol. 153*, 2592−2599.
48. Miossec, C., Decoen, M. C., Durand, L., Fassy, F., and Diu-Hercend, A. (1996) *Eur. J. Immunol. 26*, 1032−1042.
49. Cain, K., Brown, D. G., Langlais, C., and Cohen, G. M. (1999) *J. Biol. Chem. 274*, 22686−22692.
50. Bratton, S. B., Walker, G., Srinivasula, S. M., Sun, X.-M., Butterworth, M., Alnemri, E. S., and Cohen, G. M. (2001) *EMBO J. 20*, 998−1009.
51. Stennicke, H., and Salvesen, G. (2000) *Biochim. Biophys. Acta 1477*, 299−306.
52. Talanian, R. V., Quinlan, C., Trautz, S., Hackett, M. C., Mankovich, J. A., Banach, D., Ghayur, T., Brady, K. D., and Wong, W. W. (1997) *J. Biol. Chem. 272*, 9677−9682.
53. Thornberry, N. A., Rano, T. A., Peterson, E. P., Rasper, D. M., Timkey, T., Carcia-Calvo, M., Hotzager, V. M., Nordstrom, P. A., Roy, S., Vaillancourt, J. P., Chapman, K. T., and Nicholson, D. W. (1997) *J. Biol. Chem. 272*, 17907−17911.
54. Stennicke, H., Renatus, M., Meldal, M., and Salvesen, G. (2000) *Biochem. J. 350*, 563−568.
55. Cygler, M., and Mort, J. S. (1997) *Biochimie 79*, 645−652.
56. Wiederanders, B. (2000) *Adv. Exp. Med. Biol. 477*, 261−270.
57. Baker, D., Shiau, A., and Agard, D. (1993) *Curr. Opin. Cell Biol. 5*, 966−970.
58. Shi, X.-P., Chen, E., Yin, K.-C., Na, S., Garsky, V., Lai, M.-T., Li, Y.-M., Platchek, M., Register, R. B., Sardana, M. K., Tang, M.-J., Thiebeau, J., Wood, T., Shafer, J. A., and Gardell, S. J. (2001) *J. Biol. Chem. 276*, 10366−10373.
59. Butt, A. J., Harvey, N. L., Parasivam, G., and Kumar, S. (1998) *J. Biol. Chem. 273*, 6763−6768.
60. Li, Y., Hu, Z., Gordon, F., and Inouye, M. (1995) *J. Biol. Chem. 270*, 25127−25132.
61. Smith, B., and Franzen, S. (2001) *Anal. Chem.* (submitted for publication).
62. Bose, K., and Clark, A. C. (2001) *Biochemistry 40*, 14236−14242.

BI011037E